assistance with the coulometry, and S. Wang for help with figure preparation.

Supplementary Material Available: Complete listings of crystallographic data, hydrogen coordinates and isotropic parameters, anisotropic thermal parameters, and bond distances and angles (19 pages); tables of calculated and observed structure factors (17 pages). Ordering information is given on any current masthead page. Complete MSC structure reports (Nos. 88087 and 88124 for **1a** and **3**, respectively) are available on request from the Indiana University Chemistry Library.

Contribution from the Department of Chemistry, University of Illinois at Urbana-Champaign, 505 South Mathews Avenue, Urbana, Illinois 61801

High-Resolution Aluminum-27 Solid-State Magic-Angle Sample-Spinning Nuclear Magnetic Resonance Spectroscopic Study of $AlCl_3$–Tetrahydrofuran Complexes†

Oc Hee Han‡ and Eric Oldfield*

Received August 15, 1989

We have obtained ^{27}Al solid-state nuclear magnetic resonance (NMR) spectra of several $AlCl_3$–THF complexes, using "magic-angle" sample-spinning (MASS) NMR at high field. Our results suggest that the isotropic chemical shifts (δ_i) occur in relatively well defined regions for 4-, 5-, and 6-coordinate species ($AlCl_4^-$, ~103 ppm; $AlCl_3$·THF, ~99 ppm; *trans*-$AlCl_3$·2THF, ~60 ppm; *trans*-$[AlCl_2(THF)_4]^+$, ~14 ppm), as found previously with aluminum oxo compounds. We also find that theoretically calculated average nuclear quadrupole coupling constants (e^2qQ/h) (*trans*-$[AlCl_2(THF)_4]^+$, ~6.3 MHz; *trans*-$AlCl_3$·2THF, ~4.6 MHz; $AlCl_3$·THF, ~3.0 MHz; $AlCl_4^-$, 0 MHz) are in good accord with experimentally determined nuclear quadrupole coupling constants, determined from computer simulations of the MASS NMR spectra (*trans*-$[AlCl_2(THF)_4]^+$, 6.4 MHz; *trans*-$AlCl_3$·2THF, 4.9 MHz; $AlCl_3$·THF, 4.7 MHz; $AlCl_4^-$, 0.3 MHz). Both ^{27}Al δ_i and e^2qQ/h determinations appear to be useful as probes of structure in these systems, and thus offer a facile means of monitoring various solid-state reactions.

Introduction

The structure of the various complexes of aluminum chloride with organic Lewis bases has been the subject of investigation for many years, due at least in part to the fact that some aluminum complexes participate in catalytic reactions. There has been considerable interest in the $AlCl_3$–tetrahydrofuran (THF) system,[1-4] which we found of interest since it could relate to our studies of $AlCl_3$–graphite intercalation compounds—where questions as to the nature of the $AlCl_n$ complexes remain.[5] The $AlCl_3$–THF system has been extensively studied, since it can yield several kinds of complex. In the liquid state, $AlCl_3$·THF, *cis*- and *trans*-$AlCl_3$·2THF, $AlCl_4^-$, and $[AlCl_2(THF)_4]^+$ species have all been observed, and the influence of temperature, concentration, and solvent on structure has been studied. Means et al.[4] obtained only $[AlCl_4][AlCl_2(THF)_4]$ ionic crystals from a 1:2 mole ratio of $AlCl_3$ and THF in toluene, while Cowley et al.[3] obtained molecular $AlCl_3$·2THF crystals, from dissolution of $(Me_2N)_3SiCl$·$AlCl_3$ in THF. Derouault and Forel[1] also obtained ionic crystals of $[AlCl_4][AlCl_2(THF)_4]$ from a saturated solution of $AlCl_3$ in THF, and also showed that $[AlCl_4][AlCl_2(THF)_4]$ could easily lose THF in vacuo at room temperature, in the solid state, to yield a 1:1 complex $[AlCl_4][AlCl_2(THF)_4] \rightarrow 2AlCl_3$·THF + 2THF.

In this paper, we present the results of a ^{27}Al magic-angle sample-spinning (MASS) NMR study on solid-state $AlCl_3$–THF complex systems and interpret our chemical shift and quadrupole coupling constant data in structural terms, which may be of general interest.

Experimental Section

Sample Preparation. Reagent grade anhydrous Al_2Cl_6 (13.7 g, 51.4 mmol) was transferred to 137 mL of dry toluene in a 250-mL round-bottomed flask. An 18.0-mL portion of dry THF (0.207 mol) was then added, and the mixture was heated to 100 °C for 2 h under 1 atm of N_2. One portion of the product was kept at −18 ± 2 °C, and a second portion was kept at 1 ± 1 °C for about 10 h, after initial cooling to room temperature. Colorless crystals were obtained from both batches. Crystals deposited at 1 °C had a stepped-pyramidal shape and were ~7 × 7 mm at the base of the pyramid, while crystals made at −18 °C were much smaller and did not have any noticeable shape. Both sets of crystals were filtered off under N_2, and a portion of each sample was stored at −18 °C. The remainder of each sample was then kept at room temperature under N_2. The history of samples A–D can be summarized as follows: sample A was crystallized at −18 °C and kept at room temperature; sample B was crystallized at 1 °C and then kept at room temperature; sample C was crystallized at −18 °C and kept at −18 °C; sample D was crystallized at 1 °C and kept at −18 °C. We prepared $AlCl_3$·THF (sample F and a portion of sample E) by heating samples A or D at 57 °C for 5 h at ~0.1 Torr.

Nuclear Magnetic Resonance Spectroscopy. ^{27}Al MASS NMR spectra were obtained at 8.45 and 11.7 T using "home-built" spectrometers, which consist of Oxford Instruments (Osney Mead, Oxford, U.K.) 8.45-T 89-mm-bore or 11.7-T 52-mm-bore superconducting solenoid magnets, Nicolet Instrument Corp. (Madison, WI) Model 1280 computers for data acquisition, and Amplifier Research (Souderton, PA) Model 200L amplifiers for final radio frequency pulse generation. MASS NMR spectra were obtained by using a home-built probe equipped with a "Windmill"-type spinner. Samples were spun in the 6–7.5-kHz range, with less than 20 Hz of fluctuation. Chemical shifts are reported in ppm from external standards of 1 M $Al(H_2O)_6Cl_3$ aqueous solutions. More positive values correspond to low-field, high-frequency, paramagnetic or deshielded values (IUPAC δ scale). Line broadenings due to exponential multiplication were 100–200 Hz, depending on the line width.

Results and Discussion

The ^{27}Al MASS NMR spectra of samples A–D at 11.7 and 8.45 T clearly show different spectra, dependent upon sample history. For example, sample D has a main second-order powder pattern, while samples A and B have two major peaks together with numerous spinning side bands, and sample C appears to be a superposition of the spectra of samples A (or B) and D (Figure 1). The chemical shift of the resonance at ~103 ppm is field independent, and the peak has numerous first-order quadrupolar

† This work was supported in part by the Solid-State Chemistry Program of the U.S. National Science Foundation (Grant DMR 88-14789) and in part by the U.S. National Institutes of Health (Grant HL-19481).

‡ Present address: Department of Chemistry, Yale University, 225 Prospect St., New Haven, CT 06511-8118.

(1) Derouault, J.; Forel, M. T. *Inorg. Chem.* **1977**, *16*, 3207.
(2) Derouault, J.; Granger, P.; Forel, M. T. *Inorg. Chem.* **1977**, *16*, 3214.
(3) Cowley, A. H.; Cushner, M. C.; Davis, R. E.; Riley, P. E. *Inorg. Chem.* **1981**, *20*, 1179.
(4) Means, N. C.; Means, C. M.; Bott, S. G.; Atwood, J. L. *Inorg. Chem.* **1987**, *26*, 1466.
(5) Bach, B.; Ubbelohde, A. R. *Proc. R. Soc. London, A* **1971**, *325*, 437. Bach, B.; Ubbelohde, A. R. *J. Chem. Soc. A* **1971**, 3669.

0020-1669/90/1329-3666$02.50/0

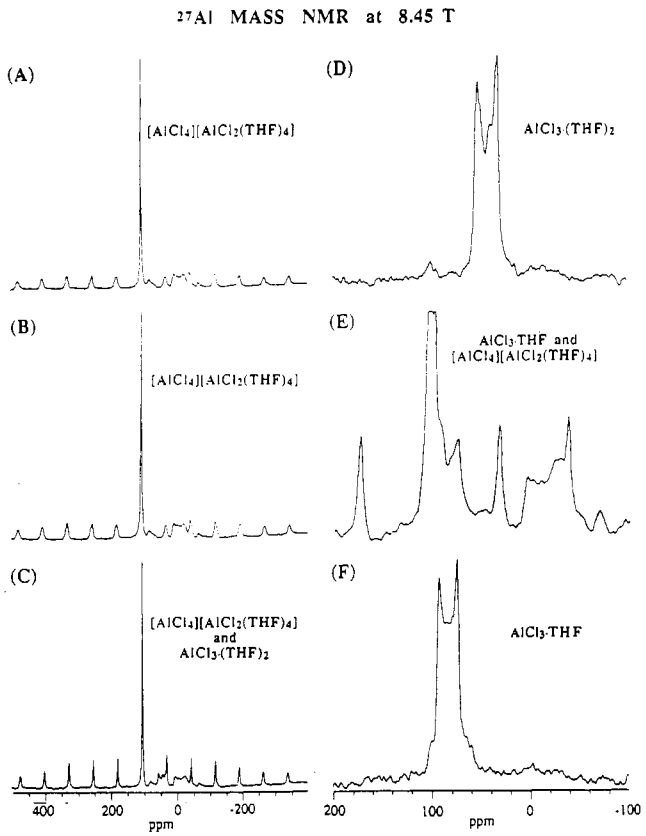

Figure 1. 8.45-T ^{27}Al MASS NMR spectra: (A) sample A, MASS at 7 kHz, 1500 scans; (B) sample B, MASS at 7 kHz, 7700 scans; (C) sample C, MASS at 6.8 kHz, 5500 scans; (D) sample D, MASS at 6.8 kHz, 6200 scans; (E) sample E, MASS at 6.6 kHz, 4200 scans; (F) sample F, MASS at 6.8 kHz, 3200 scans. Recycle time was 300 ms for all spectra.

spinning sidebands. The quadrupole coupling constant is ~300 ± 50 kHz, and this peak can readily be assigned to the well-known species $AlCl_4^-$. The nonzero e^2qQ/h value implies that $AlCl_4^-$ has a slightly distorted tetrahedral structure, in the solid state.

The broad resonance observed near 0 ppm in Figure 1A,B,C,E exhibits a second-order quadrupolar powder pattern, and is a $^1/_2$, $-^1/_2$ transition (from nutation experiments). Figure 2A shows a computer simulation yielding $\delta_i = 14 \pm 1$ ppm, $e^2qQ/h = 6.4 \pm 0.1$ MHz, and $\eta = 0$. This resonance is assigned to $[AlCl_2(THF)_4]^+$ on the basis of chemical analysis and the observation of the $AlCl_4^-$ peak (at 103 ppm). The fact that $\eta = 0$ shows that this species is axially symmetric, and the isotropic chemical shift near 0 ppm strongly suggests octahedral coordination. While both *cis* and *trans*-$[AlCl_2(THF)_4]^+$ will be expected to resonate in the ~0 ppm chemical shift range and will have $\eta = 0$, the cis isomer is ruled out on the basis of the observed e^2qQ/h value, as discussed below in more detail. Our results thus indicate that samples A and B are $[AlCl_4]$[*trans*-$AlCl_2(THF)_4$].

The powder pattern of sample D (Figure 1D) can be assigned to the *trans*-$AlCl_3$·2THF isomer over the other two possible five-coordinate forms shown in Figure 3 on the basis of the NMR results, which show an axially symmetric species in a chemical shift range midway between that of the 4- and 6-coordinate systems. We believe it to be the 5-coordinate species, on the basis of the general deshielding of the chloro complexes over that found in Al–O species.[6] From the spectral simulation given in Figure 2B, we find $\delta_i = 60 \pm 1$ ppm, $e^2qQ/h = 4.9 \pm 0.3$ MHz, $\eta = 0.05 \pm 0.05$. Our assignment is consistent with the expectation that steric interactions between the THF ligands are minimized in the trans isomer.

(6) (a) Engelhardt, G.; Michel, D. *High-Resolution Solid-State NMR of Silicates and Zeolites*; John Wiley & Sons: New York, 1987. (b) In *NMR of Newly Accessible Nuclei*; Laszlo, P., Ed.; Academic Press: New York, 1983; Vol. 2, Chapter 6.

Table I. Electric Field Gradient Tensor Invariant (g_ϕ^2), Electric Field Gradient (eq), and Electric Field Gradient Tensor Asymmetry Parameters (η), for Tetrahedral and Octahedral Complexes, Computed by Using a Point Charge Model

complex	sym	$g_\phi^{2\,a}$	eq^b	η^c
		Tetrahedral[d]		
MX_4 (MY_4)	T_d	0	0	0
MX_3Y (MXY_3)	C_{3v}	$9\left(\frac{e_x}{R_x^3}-\frac{e_y}{R_y^3}\right)^2$	$-2\left(\frac{e_x}{R_x^3}-\frac{e_y}{R_y^3}\right)$	0
MX_2Y_2	C_{2v}	$12\left(\frac{e_x}{R_x^3}-\frac{e_y}{R_y^3}\right)^2$	$\pm 2\left(\frac{e_x}{R_x^3}-\frac{e_y}{R_y^3}\right)$	1
		Octahedral[d]		
MX_6 (MY_6)	O_h	0	0	0
MX_5Y (MXY_5)	C_{4v}	$9\left(\frac{e_x}{R_x^3}-\frac{e_y}{R_y^3}\right)^2$	$-2\left(\frac{e_x}{R_x^3}-\frac{e_y}{R_y^3}\right)$	0
trans-MX_4Y_2 (MX_2Y_4)	D_{4h}	$36\left(\frac{e_x}{R_x^3}-\frac{e_y}{R_y^3}\right)^2$	$-4\left(\frac{e_x}{R_x^3}-\frac{e_y}{R_y^3}\right)$	0
cis-MX_4Y_2 (MX_2Y_4)	C_{2v}	$9\left(\frac{e_x}{R_x^3}-\frac{e_y}{R_y^3}\right)^2$	$2\left(\frac{e_x}{R_x^3}-\frac{e_y}{R_y^3}\right)$	0
mer-MX_3Y_3	C_{2v}	$27\left(\frac{e_x}{R_x^3}-\frac{e_y}{R_y^3}\right)^2$	$\pm 3\left(\frac{e_x}{R_x^3}-\frac{e_y}{R_y^3}\right)$	1
fac-MX_3Y_3	C_{3v}	0	0	0

[a] Electric field gradient tensor invariant expressed by using ligand charges, e_x and e_y, and corresponding ligand distances from the central metal ion M, R_x and R_y. [b] Electric field gradient $eq \equiv \phi_{zz} = V_{zz}$ in the principal-axis system. The sign of eq is as shown for MX_mY_{n-m} with $m \geq (n-m)$, and opposite for $m < (n-m)$. [c] Electric field gradient tensor asymmetry parameters: $\eta = (V_{xx} - V_{yy})/V_{zz}$, where $|V_{zz}| \geq |V_{yy}| \geq |V_{xx}|$. [d] If a ligand "n" is changed from a point charge e_n to a dipole d_n, replace e_n in the table with $(\pm)3d_n/R_n$, depending on the orientation of the dipole.

Our results thus indicate that samples A and B are $[AlCl_4]$-[*trans*-$AlCl_2(THF)_4$], that sample D is *trans*-$AlCl_3$·2THF, and that sample C is an admixture of $AlCl_3$·2THF and $[AlCl_4][AlCl_2(THF)_4]$.

The effect of temperature on the equilibrium $[AlCl_4][AlCl_2(THF)_4] \leftrightarrow 2(AlCl_3 \cdot 2THF)$ was reported by Derouault et al. in the liquid state,[2] the concentration of ionic species increasing at lower temperatures. We believe the same equilibration reaction may hold in our system (even with toluene as solvent), resulting in $AlCl_3$·2THF (sample D, crystallized at 1 °C) or the mixture $AlCl_3$·2THF and $[AlCl_4][AlCl_2(THF)_4]$ (sample C, crystallized at −18 °C).

When Al_2Cl_6·4THF ($AlCl_3$·2THF or $[AlCl_4][AlCl_2(THF)_4]$) samples were dried in a vacuum oven at 57 °C for 5 h, the final product, $AlCl_3$·THF (composition confirmed by microanalysis), gave the same ^{27}Al MASS NMR spectrum (Figure 1F) regardless of starting materials, i.e. $AlCl_3$·2THF or $[AlCl_4][AlCl_2(THF)_4]$, or a mixture of both. From the spectral simulation given in Figure 2C, we find $\delta_i = 99 \pm 1$ ppm, $e^2qQ/h = 4.7 \pm 0.2$ MHz, and $\eta = 0$, consistent with a tetrahedral formulation, $AlCl_3$·THF. Sample E was made by partial removal of THF from $AlCl_3$·2THF (sample D), and the spectrum exhibits resonances for $AlCl_3$·THF and $[AlCl_4][AlCl_2(THF)_4]$ but has no resonance for $AlCl_3$·2THF (see e.g. Figure 1D,E). Thus, removal of THF by heating in vacuo may occur via the isomerization step

$$AlCl_3 \cdot 2THF \rightarrow [AlCl_4][AlCl_2(THF)_4] \rightarrow 2(AlCl_3 \cdot THF) + 2THF \quad (1)$$

Nuclear Quadrupole Coupling Constants

We now comment in more detail on the e^2qQ/h values we have observed in our complexes, since the actual magnitudes of e^2qQ/h

Table II. Electric Field Gradient Tensor Components for 5-Coordinate Bipyramidal Complexes

complex[a]	sym	ϕ_{ii}[b]	ϕ_{jj}[b]	ϕ_{kk}[b]
MX_5 (MY_5)	D_{3h}	$\frac{e_x}{R_x^3}$	$-\frac{1}{2}\frac{e_x}{R_x^3}$	$-\frac{1}{2}\frac{e_x}{R_x^3}$
axial-MX_4Y (MY_4X)	C_{3v}	$-\frac{e_x}{R_x^3}+2\frac{e_y}{R_y^3}$	$\frac{1}{2}\frac{e_x}{R_x^3}-\frac{e_y}{R_y^3}$	$\frac{1}{2}\frac{e_x}{R_x^3}-\frac{e_y}{R_y^3}$
equatorial-MX_4Y (MY_4X)	C_{2v}	$2\frac{e_x}{R_x^3}-\frac{e_y}{R_y^3}$	$\frac{1}{2}\frac{e_x}{R_x^3}-\frac{e_y}{R_y^3}$	$-\frac{5}{2}\frac{e_x}{R_x^3}+2\frac{e_y}{R_y^3}$
trans-MX_3Y_2 (MY_3X_2)	D_{3h}	$-3\frac{e_x}{R_x^3}+4\frac{e_y}{R_y^3}$	$\frac{3}{2}\frac{e_x}{R_x^3}-2\frac{e_y}{R_y^3}$	$\frac{3}{2}\frac{e_x}{R_x^3}-2\frac{e_y}{R_y^3}$
diequatorial-MX_3Y_2 (MY_3X_2)	C_{2v}	$3\frac{e_x}{R_x^3}-2\frac{e_y}{R_y^3}$	$-3\frac{e_x}{R_x^3}+\frac{5}{2}\frac{e_y}{R_y^3}$	$-\frac{1}{2}\frac{e_y}{R_y^3}$
axial–equatorial-MX_3Y_2 (MY_3X_2)	Cs	$\frac{e_y}{R_y^3}$	$\frac{3}{2}\frac{e_x}{R_x^3}-2\frac{e_y}{R_y^3}$	$-\frac{3}{2}\frac{e_x}{R_x^3}+\frac{e_y}{R_y^3}$

[a] MX_5, *axial*-MX_4Y, and *trans*-MX_3Y_2 have $\phi_{zz}=\phi_{ii}$, $\eta=0$, and $\phi_g^2=(9/4)\phi_{zz}^2$. For the other cases, ϕ_{zz} depends on the relative values of e_x/R_x^3 and e_y/R_y^3. [b] ϕ_{pp} where $p=i,j,k$ are ϕ_{xx}, ϕ_{yy}, and ϕ_{zz} in PAS. The ϕ_{pp} having the largest absolute value is $\phi_{zz}=eq$, and the other two are ϕ_{xx} and ϕ_{yy}, depending on the relative values of e_x/R_x^3 and e_y/R_y^3.

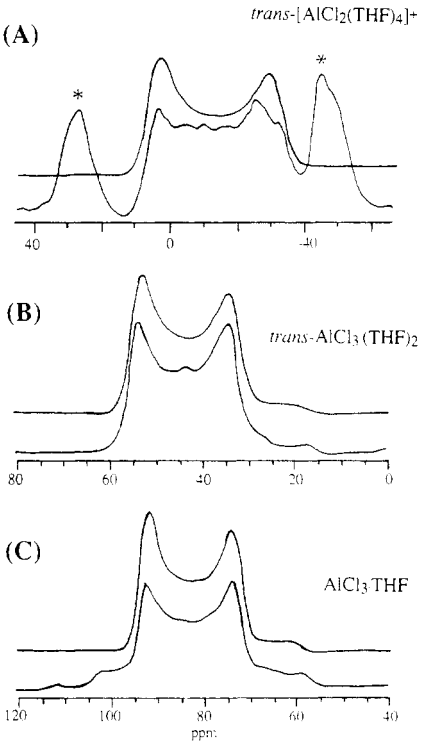

Figure 2. Second-order quadrupolar powder pattern simulations (top part of each figure): (A) *trans*-$[AlCl_2(THF)_4]^+$ with δ_i = 13.5 ppm, QCC = 6.5 MHz, and η = 0 (asterisk indicates spinning sidebands of the $AlCl_4^-$ component); (B) *trans*-$AlCl_3$·2THF with δ_i = 60 ppm, QCC = 4.95 MHz, and η = 0; (C) $AlCl_3$·THF with δ_i = 98 ppm, QCC = 4.8 MHz, and η = 0.

can give useful structural information.

There have previously been a number of papers outlining the theory of quadrupolar relaxation in e.g. ^{27}Al complexes[7,8] and of other related systems, e.g. ^{59}Co[9,10] and ^{93}Nb complexes.[11] It is well-known, for example, that *fac*-octahedral complexes have small g_ϕ^2 values for the central metal ion (or long T_1 and T_2 values), while the corresponding *mer*-octahedral complexes have large g_ϕ^2 values and short T_1 and T_2 values (in solution). A number of workers[7-11] have estimated the effects of substitution in octahedral complexes, using point charge models.

We have carried out similar calculations for our 4-, 5-, and 6-coordinate complexes, using point charge and/or point dipole models, and our results for tetrahedral and octahedral systems are shown in Table I. For the octahedral complexes, our results for the electric field gradient (EFG), *eq*, are in good agreement with the relative values found by Yamasaki et al.,[9] as well as those derived in the context of Mössbauer spectroscopy by Clark.[12] However, our results for *cis*- and *trans*-$MX_4Y_2(MX_2Y_4)$ are at variance with the results obtained by Tarasov et al.,[11] quoted by Wehrli and Wehrli.[8]

In Mössbauer spectroscopy, the ratio of the EFG (or quadrupole splitting) for certain *cis*- and *trans*-FeX_4Y_2 complexes has been found to be 2(trans):−1(cis),[13] and this is the theoretical result deduced by Clark,[12] and is in agreement with that which can be deduced by a point charge model,[7,10] as shown in Table I. Specifically then

$$e^2qQ/h(\text{trans}) = -2e^2qQ/h(\text{cis}) \quad (2)$$

For the EFG tensor invariant, g_ϕ^2, we expect

$$g_\phi^2(\text{trans}) = 4g_\phi^2(\text{cis}) \quad (3)$$

since

$$g_\phi^2 = \frac{9}{4}\left(1+\frac{\eta^2}{3}\right)\phi_{zz}^2 \quad (4)$$

and $\eta = 0$ for both stereoisomers. However, Tarasov et al.[11] and Wehrli and Wehrli[8] find the ratio to be ~2.25 rather than 4, which is at variance with our point charge calculation, the point charge calculation of Yamasaki et al.,[9] the Mössbauer experiments,[13] and the irreducible tensor formulation of Clark.[12] The experimentally observed solution NMR line width ratios are somewhere in between, but any nonquadrupolar broadening (due e.g. to chemical shift anisotropy, dipolar interactions, or chemical exchange) will mask the large differential line widths expected from theory.

For 5-coordinate complexes, we have calculated the individual EFG tensor components, ϕ_{ii}, and the results are given in Table II.

(7) Valiyev, K. A.; Zripov, M. M. *Zh. Strukt. Khim.* **1966**, *7*, 494.
(8) Wehrli, F. W.; Wehrli, S. *J. Magn. Reson.* **1981**, *44*, 197.
(9) Yamasaki, A.; Yajima, F.; Fujiwara, S. *Inorg. Chim. Acta* **1968**, *2*, 39.
(10) Yajima, F.; Koike, Y.; Yamasaki, A.; Fujiwara, S. *Bull. Chem. Soc. Jpn.* **1974**, *47*, 1442.
(11) Tarasov, V. P.; Privalov, V. I.; Buslaev, Yu. A. *Mol. Phys.* **1978**, *35*, 1047.
(12) Clark, M. G. *Mol. Phys.* **1971**, *20*, 257.
(13) Berrett, R. R.; Fitzsimmons, B. W. *J. Chem. Soc. A* **1967**, 525. Bancroft, G. M.; Mays, M. J.; Prater, B. E. *J. Chem. Soc., Chem. Commun.* **1968**, 1374. Bancroft, G. M.; Garrod, R. E. B.; Maddock, A. G.; Mays, M. J.; Prater, B. E. *J. Chem. Soc., Chem. Commun.* **1970**, 200.

Table III. Experimental ^{27}Al Chemical Shift, Quadrupole Coupling Constant, and Electric Field Gradient Tensor Asymmetry Parameters and Calculated Quadrupole Coupling Constants for $AlCl_3$–THF Complexes and Model Compounds

complex	δ_i,[a] ppm	$\lvert e^2qQ/h\rvert$,[b] MHz	η[c]	e^2qQ/h(computed), MHz		
				d	*e*	*f*
$AlCl_3$·THF	99	4.7 ± 0.2	0	3.59	2.94	2.58
trans-$AlCl_3$·2THF	60	4.9 ± 0.3	0.05	5.39	5.03	3.34
diequatorial-$AlCl_3$·2THF				±5.39	4.31	−4.31
axial–equatorial-$AlCl_3$·2THF				±2.76	−2.51	2.23
$AlCl_4^-$	103	0.3 ± 0.05	0	0	0	0
trans-$[AlCl_2(THF)_4]^+$	14	6.4 ± 0.1	0	−7.54	−6.46	−5.03
cis-$[AlCl_2(THF)_4]^+$				3.59	3.20	2.58
$AlCl_4^-$ in $Na^+[AlCl_4]^-$	100					
$AlCl_4^-$[g]	102					
$AlCl_3$·2THF[g]	63					
$[AlCl_2(THF)_4]^+$[g]	16					

[a] Isotropic chemical shift, in ppm from 1 M $Al(H_2O)_6Cl_3$. Error is ±1 ppm. [b] Experimental nuclear quadrupole coupling constant. [c] Experimental electric field gradient tensor asymmetry parameter. [d] Computed nuclear quadrupole coupling constant, assuming $e_{THF} = 0$, $e_{Cl} = e$. [e] Computed nuclear quadrupole coupling constant obtained by using point charges calculated with a Gaussian-85 program. [f] Computed nuclear quadrupole coupling constant, assuming $d_{THF} = 1.63$ D, $e_{Cl} = e$. The "bond" lengths used were average values obtained from the X-ray refinements. The bond angles used were ideal values. [g] Isotropic ^{27}Al chemical shifts of $AlCl_3$ in THF(l).

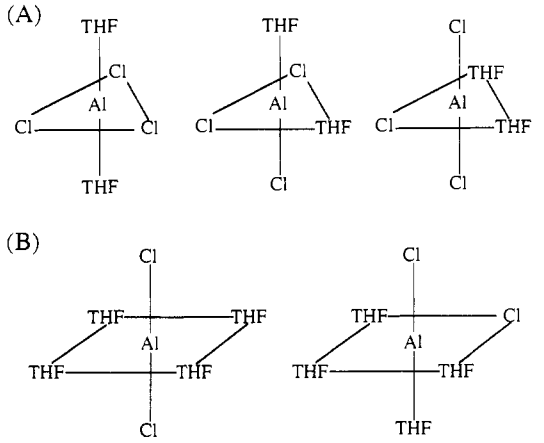

Figure 3. (A) Stereoisomers of $AlCl_3$·2THF: trans or diaxial isomer, axial–equatorial isomer, and diequatorial isomer, from left to right. (B) Stereoisomers of $[AlCl_2(THF)_4]^+$: trans isomer and *cis*-isomer, from left to right.

From the individual EFG components given in Tables I and II, we have calculated the expected quadrupole coupling constants for ^{27}Al, using the relation

$$e^2qQ/h = (1 + \gamma_\infty)eQ\cdot V_{zz} = (1 + \gamma_\infty)eQ\cdot eq \qquad (5)$$

where γ_∞ is the ^{27}Al Sternheimer antishielding factor (=2.59; from refs 7, 14), eQ is the nuclear quadrupole moment, and eq is the computed electric field gradient (V_{zz}). Table III gives results for each of the complexes investigated, together with comparison values for some alternative possible structures, computed with assumptions of (i) a zero charge for THF, (ii) the estimated dipole moment of THF, or (iii) effective charges calculated via an ab initio procedure (using a Gaussian-85 program). There is clearly good agreement between experiment and each of the three calculations, with *cis*- and *trans*-$[AlCl_2(THF)_4]^+$ being clearly differentiated on the basis of the very large observed e^2qQ/h value (Table III).

Such good agreement between theory and experiment is possibly to some extent fortuitous, since distortion from ideal geometry, uncertainties in bond lengths, long-range effects from nonbonded ligands, and the assumption of the addition of the electric field gradients are all assumptions inherent in the model used. Thus, it would always be wise to use observed e^2qQ/h and η values of unknown systems in combination with calculations *and* additional measurements on systems having known structures, in order to make definitive structural statements. Nevertheless, we believe that the results we have presented above indicate that combined measurement of isotropic chemical shifts, nuclear quadrupole coupling constants, and asymmetry parameters via solid-state NMR spectroscopy appears to be quite useful as a technique for monitoring the reactivity and rearrangement of Lewis acid–base adducts and may also be helpful for analyzing other multicomponent or noncrystalline systems as well.

Acknowledgment. We thank Y. C. Moon for helping to synthesize the samples, D. C. Lim for calculation of point charges using a Gaussian-85 program, and Dr. J. Haase for helpful comments.

(14) Cohen, M. H.; Reif, F. *Solid State Phys.* **1957**, *5*, 321.